

HYDROTHERMAL SYNTHESIS OF NANOSIZED HETEROATOM AND Fe DOPED-TiO₂ AS PHOTSENSITIVE MATERIALS FOR SOLAR HYDROGEN GENERATION

A. M. MURUGAN^{a*}, R. R. JOTHI^b, K. R. ANJU^c, A. A. IBRAHIM AHAMED^a, T. RADHIKA^c

^a*Department of Botany and Microbiology, College of Science, King Saud University, Riyadh, Saudi Arabia.*

^b*Chemistry Department, College of Science, King Saud University, P.O. Box 2455, Riyadh 11451, Saudi Arabia.*

^c*Centre for Materials for Electronics Technology [C-MET, DietY], Athani P.O., Thrissur-680581, India.*

Photosensitive N-TiO₂ and Fe-N-TiO₂ materials were prepared through hydrothermal method. The XRD pattern shows only characteristic peaks of anatase TiO₂ and further confirmed by Raman spectra. The crystallite size of the materials is in the range of 20-25 nm and is also confirmed from TEM. DR UV-Vis pattern shows a shift in the absorption to the visible region for N and Fe-N doped materials compared to TiO₂. Photosensitive studies conducted using methylene blue dye in an immersion type photoreactor under visible lamp confirmed increased degradation activity for the doped materials. These materials are promising for the generation of hydrogen fuel through water splitting in presence of solar energy.

(Received March 29, 2017; Accepted September 28, 2017)

Keywords: Hydrothermal, Water splitting, Solar hydrogen, N-TiO₂, Fe-N-TiO₂, Methylene blue

1. Introduction

Photosensitive water splitting is one of the best routes for solar-hydrogen, *the future fuel* generation. Most of the investigations have focused on TiO₂, which shows relatively high activity and chemical stability under UV light irradiation. It is a well known photocatalyst and is very sensitive towards several applications such as self-cleaning, dye sensitized solar cells etc. [1,2]. The major drawback of TiO₂ lies in its ineffective use of visible light because of its wide band gap (3.2 eV). There is an urgent need to develop photosensitive materials that can yield high activity under visible light. The incorporation of certain dopants in TiO₂ should increase its activity either by creating new band structures or by suppressing the recombination of electron hole pairs resulting in high quantum efficiency [7]. Hydrothermal method is one of the unique methods for synthesizing materials with high purity, narrow particle size distribution and controlled morphology. In the present work, N-TiO₂ and Fe-N-TiO₂ materials were prepared through hydrothermal method and investigated its structure using various physico-chemical techniques. Initial photosensitive activity studies were conducted using methylene blue dye in an immersion type photoreactor under visible lamp in view to extent to solar hydrogen generation applications.

2. Experimental

Titanium (IV) butoxide [Ti(OC₄H₉)₄, TBO, [AR, Sigma Aldrich] was hydrolysed using dH₂O, transferred into a Teflon lined autoclave and placed in an oven at 433 K for 6 h. The

*Corresponding author: ammurugan11@gmail.com

material was centrifuged, dried at 353 K and calcined at 773 K for 3 h to get TiO_2 . To prepare N- and Fe-N- TiO_2 , the same procedure was followed with the addition of NH_3 solution ($x\text{N:T}$, $x=0.25, 0.5$ and 1.0 molar ratio) and $\text{Fe}(\text{NO}_3)_3 \cdot 9\text{H}_2\text{O}$ (Merck). The materials were characterized using Powder X-ray diffraction (AXS Bruker D5005 X-ray diffractometer), Raman spectroscopy (DSR Raman microscope) and DR-UV Visible spectroscopy (JASCO UV-Visible spectrophotometer V550 ISV469). Degradation of methylene blue was carried out in an immersion type photoreactor with visible light (300W Visible 230V AC) and studied using UV-Visible spectrophotometer (Perkin Elmer-USA model Lambda 35).

3. Results and discussion

The powder X-Ray diffraction patterns of the prepared materials are shown in Fig. 1. The XRD pattern shows only crystalline anatase TiO_2 phase in all the materials without any additional peaks in N- TiO_2 and Fe-N- TiO_2 [5]. For N- TiO_2 , the crystallite size lies in the range of ~ 22 - 25 nm. However, for Fe-N- TiO_2 , the crystallite size increased to 32 nm.

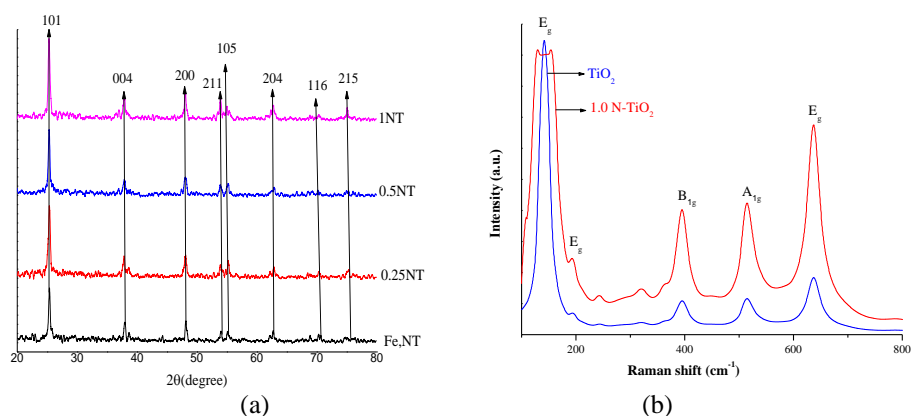


Fig. 1. (a) Powder X-Ray diffraction pattern and (b) Raman spectra

In Figure 1 (b) the observed Raman active modes are characteristic of anatase TiO_2 assigned to E_g and B_{1g} modes which confirms the XRD pattern [6,7]. FT-IR spectra and TG-DSC of the materials confirms the complete removal of organics at the calcination temperature to form TiO_2 network [5,7].

Fig. 2 (a) depicts the DR-UV-Vis spectra of the prepared materials calcined at 773K. The spectra shows red shift as the ratio of N:Ti increases. Fig. 2 (b) represents the tauc plot of the materials.

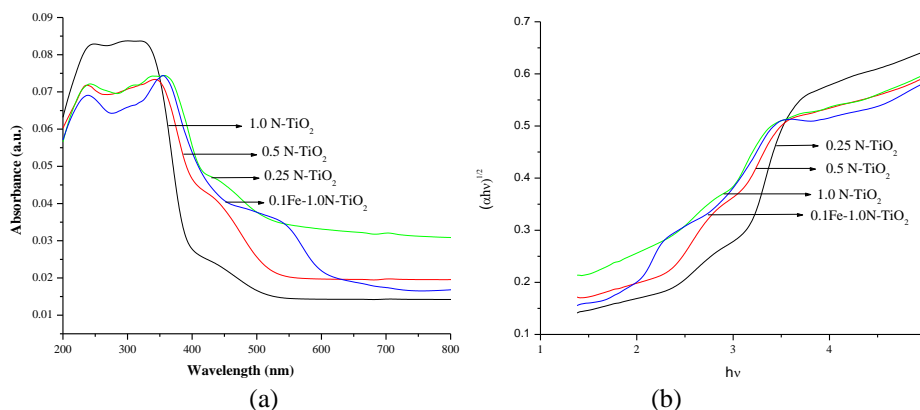


Fig. 2. (a) DR UV-Vis spectra and (b) Tauc plot of the materials.

The band gap energies are listed in Table 3.1. The band gap energy for anatase TiO₂ is 3.2 eV. A decrease in the band gap energy is observed for the N doped TiO₂ and a further decrease is observed for the Fe, N codoped TiO₂. All the N-TiO₂ materials show red shift towards visible light region, suggesting the formation of an energy level within the band gap [7,9-10]. Moreover, the absorption in this range increases with the increase in doped N content.

Table 1. Band gap energy and λ_{max} of the materials

Sl. No:	Material prepared	λ_{max}	Band gap energy (eV)	
			Calculated	Tauc plot
1.	0.25N-TiO ₂	473	2.62	2.64
2.	0.5N-TiO ₂	526	2.35	2.20
3.	1.0N-TiO ₂	590	2.09	2.01
4.	0.1Fe1.0N-TiO ₂	602	2.05	1.99

The photosensitive activity of the prepared materials was studied using Methylene blue (MB) dye in visible light in an immersion type photoreactor (Fig. 3).

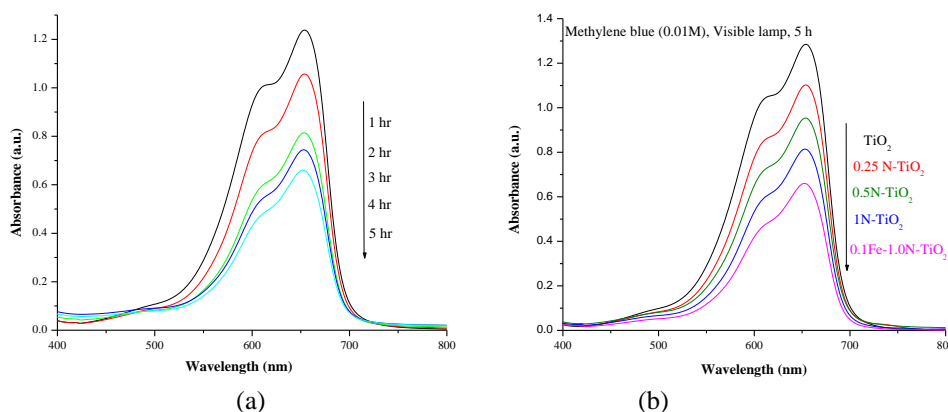


Fig. 3. Methylene blue absorption spectra of (a) 1.0N-TiO₂ and (b) all materials at 5h.

The materials show good activity under visible light. The degradation of MB was increased as the time of exposure increased. Degradation occurs by the reaction of electrons and holes generated by the materials with MB [11-15]. Methylene blue is a potential model compound and it's a cationic dye with two intense absorption bands usually appeared at 290 and 661 nm ranges. The absorption at 661 nm belongs to the orange region and that is the reason it appeared as dark blue coloured. The visible range has two peaks around at 610 and 660 nm due to the formation Methylene blue dimers and monomer respectively. Generally absorption spectrum shows only absorption corresponding to MB monomer at 660 nm. The photosensitive action of different mole ratio of doped (N-TiO₂ and Fe-N-TiO₂) photo catalyst are tested for Methylene blue degradation/decolouration reaction under direct solar light irradiation. The degradation leads to the gaseous product as well as formation of harmless small molecules such as inorganic anions such as nitrate, chloride, sulphate molecules etc. The reaction taking place during the degradation of MB can be represented as below;



The UV spectra of Methylene blue degradation with modified N-TiO₂ NPs photo catalyst are shown in Fig. 4A and 4B at various time duration upto 6 h. The observed reduction in MB concentration under direct sunlight in presence of prepared materials confirms the photosensitive

activity of the N-TiO₂ based materials at 4 h, the degradation rate of Methylene blue solution is more for the N-TiO₂ materials than TiO₂ i.e., the characteristic absorption bands of Methylene blue solution at 610 nm were significantly lower the peak intensity for the N doped TiO₂ nanoparticles. It suggests that the nitrogen doping level has a typical influence on the photocatalytic activity. The absorbance spectrum of a blank MB solution without any photosensitive material kept in the dark shows no degradation at all. Another Methylene blue solution kept in the light without any photosensitive materials shows very little reduction in intensity after 4 h. It is observed that the degradation is more effective for the material with higher concentration of nitrogen doping on TiO₂ lattice.

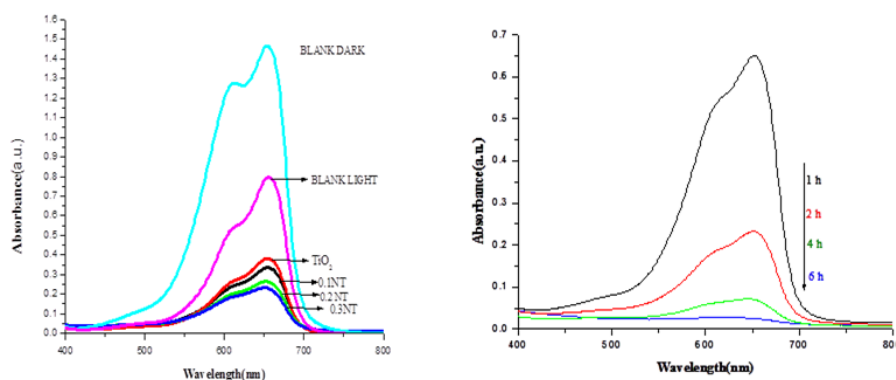


Fig. 4. Degradation of MB (A) 0.1 N-TiO₂ (B) Degradation of MB using 0.2 N-TiO₂ at different time of exposure

This is due to the fact that the photosensitive action of the materials under solar light increases when the nitrogen get doped into the materials since it can shift the absorption edge of the materials to the visible region than undoped TiO₂. Fig 7 B shows the degradation of MB solution in presence of 0.2NT as a function of time. As the time increases the degradation also increases and at 6h, MB is completely degraded as indicated by the very less intense absorption pattern in the visible region. The degradation of MB occurs by the reaction of electrons and holes generated by the photosensitive materials with MB. The fast degradation of MB solution occurs on NT materials is due to the effective absorption of solar energy by the NT materials and thus reduce the electron-hole recombination. This will enhance the photosensitive activity of the prepared materials. Figure 8 shows the combined results of enhanced activity of photosensitive material like N-TiO₂ NPs and Fe-N-doped TiO₂ NPS for effective or complete decolouration after 6 h of time duration under direct solar radiation.

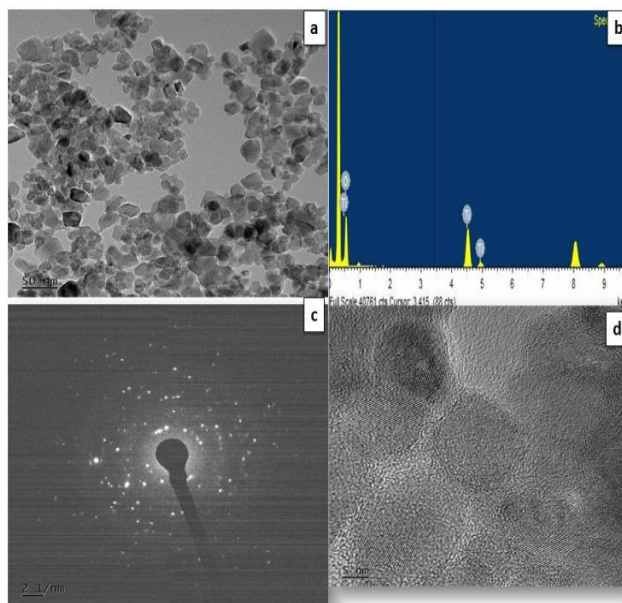


Fig 5 TEM images of Fe-N-TiO₂

The fine nanoparticle N and Fe doped TiO₂ NPs are confirmed by TEM analysis and SEM analysis. Figure 4 and 5 shows the TEM-EDX of TiO₂ nanoparticle and N-TiO₂ nanoparticle, due the preparation methodology adopted in the present study causes fine rectangle and square shape morphology for N-TiO₂ nanoparticles. The particle formed in the range 5-10 nm size and decrease in particle size could provide the active surface sites for absorbing species and alter the inner energy levels of the TiO₂ band structure. The SEM micrographs of Fe-N-TiO₂ nanoparticles with fine shaped morphology and its also confirms the closer particle morphology with similar shape observed below 100 nm scale (not shown here). Light scattering particle size analysis is further confirm the average particle size for Fe-N-TiO₂ nanoparticles, which is observed below 5 nm range (Fig. 5a and 5b) and it could be the exiting result for the field TiO₂ nanoparticles fabrication towards catalysis and dye sensitized solar cell applications.

4. Conclusions

The powder X-ray diffraction patterns of all the materials show crystalline anatase TiO₂ with crystallite size in the range of ~20-25 nm. In Raman spectra, modes corresponding to anatase TiO₂ only observed which confirms the XRD pattern. From DR UV-Vis studies, the extension of absorption spectra into visible region (red shift) suggests reduced band gap for doped TiO₂. The codoping of N with Fe further reduces the band gap energy to a lower value. Average particle size for Fe-N-TiO₂ sample was observed at 12 nm. Very fine reactangle shaped nanoparticle formed for Fe-N-TiO₂ photo catalyst. This will enhance the visible absorption ability of the materials which is proved by the degradation studies on methylene blue. These materials are finds promising for hydrogen generation by making use of solar energy.

Acknowledgement

The authors are grateful to Deanship of Scientific Research at King Saud University for its funding of this research through the Research Group project Number- (RG-1435-057).

References

- [1] G. Yang, Z. Jiang, H. Shi, T., Xiao Z. Yan, *J. Mater. Chem* **20**, 5301 (2010).
- [2] Y.G. Kang, K.H. Lee, H.S. Hahm, *Turk. J. Chem.* **39**, 159 (2015).
- [3] M.M. Joshi, P. A. Mangrulkar, S. N. Tijare, P. S. Padole, D. V. Parwate, K. L Nitin, S. S. Rayalu, *Inter. J. Hydrogen Energy* **37**, 10457 (2012).
- [4] J. X. Feng Wang, W. Liu, W. Cao, *Inter. J. Photoenergy*, , 1-7. 2013
- [5] Y.Z. Yu-Chang Liu, Y. F. Lu, J. C. Chung, *Inter. J. Chem. Eng. Appl.* **3**, 234 (2014).
- [6] S.H. Liu, Siu H.R., *Appl. Energy* **100**, 148 (2012).
- [7] I. Ganesh, P. P. Kumar, A. K. Gupta, P.S.C. Sekhar, K. Radha, G. Padmanabham, G. Sundararajan, *Proce. Appl. Ceram.* **1**, 21 (2012).
- [8] M. Factorovich, L. Guz, R. Candal, *Adv. Phys. Chem.*, 2011, Article ID 821204.
- [9] T.P. Dhanya, S. Sugunan, *J. App. Chem.* **3**, 27 (2013).
- [10] N.G. Moustaka, A.G. Kondos, V. Likodimos, F. Katsaros, *Appl. Cata. B: Environ.* **14**, 130 (2013).
- [11] D. Cheng, Z. Jiang, J. Geng, Q. Wang, D. Yang, *Ind. Eng. Chem. Res.* **46**, 2741 (2007).
- [12] L. Szatmáry, S. Bakardjieva, J. Subrt, P. Bezdicka, J. Jirkovsky, Z. Bastl, V. Brezová, M. Korenko, *Catal. Today* **161**, 23 (2011).
- [13] G. Zhang, Y. C. Zhang, M. Nadagouda, C. Han, K. O'Shea, S.M. El-Sheikh, A. A. Ismail, D. D. Dionysiou, *Appl. Catal. B: Environ.* **144**, 614 (2014).
- [14] X. Chen, S.S. Mao, *Chem. Rev.* **107**, 2891 (2007).
- [15] C. Di Valentin, E. Finazzi, G. Pacchioni, A. Selloni, S. Livraghi, M.C. Paganini, E. Giamello, *Chem. Phys.* **339**, 44 (2007).